

Thermodynamic Measurement of Angular Anisotropy at the Hidden Order Transition of URu₂Si₂

Jennifer Trinh¹, Ekkes Brück², Theo Siegrist^{3,4}, Rebecca Flint⁵,

Premala Chandra⁶, Piers Coleman^{6,7} and Arthur P. Ramirez¹

¹ *Physics Department, UC Santa Cruz, Santa Cruz, California, 95064, USA*

² *Fundamental Aspects of Materials and Energy, Faculty of Applied Sciences, TU Delft Mekelweg, 15, 2629 JB, Delft, The Netherlands*

³ *National High Magnetic Field Laboratory, Florida State University, Tallahassee, Florida, 32310, USA*

⁴ *Department of Chemistry and Biomedical Engineering, Florida State University, Tallahassee, Florida, 32310, USA*

⁵ *Department of Physics and Astronomy, Iowa State University, Ames, Iowa, 50011 and*

⁶ *Center for Materials Theory, Rutgers University, Piscataway, New Jersey, 08854, USA*

⁷ *Department of Physics, Royal Holloway, University of London, Egham, Surrey TW20 0EX, UK*
(Dated: August 26, 2016)

The heavy fermion compound URu₂Si₂ continues to attract great interest due to the unidentified hidden order it develops below 17.5K. The unique Ising character of the spin fluctuations and low temperature quasiparticles is well established. We present detailed measurements of the angular anisotropy of the nonlinear magnetization that reveal a $\cos^4\theta$ Ising anisotropy both at and above the ordering transition. With Landau theory, we show this implies a strongly Ising character of the itinerant hidden order parameter.

Despite intensive theoretical and experimental efforts, the hidden order (HO) that develops below 17.5K in the heavy fermion superconductor URu₂Si₂ remains unidentified thirty years after its original discovery [1]. The nature of the quasiparticle excitations and the broken symmetries associated with the HO phase are important questions for understanding not only HO but also the low-temperature exotic superconductivity. While URu₂Si₂ is tetragonal above the HO, torque magnetometry [2], cyclotron resonance[3], x-ray diffraction [4] and elastoresistivity measurements [5] indicate fourfold symmetry-breaking in the basal plane. However NMR and NQR studies suggest that this nematic signal decreases with increasing sample size and also depends on sample quality, suggesting that the bulk is tetragonal [6, 7].

A number of measurements on URu₂Si₂ indicate Ising anisotropy, suggesting that it is essential to understanding its HO. At the HO transition temperature T_c , both the linear (χ_1) and nonlinear (χ_3) susceptibilities are anisotropic, with χ_3 displaying a sharp anomaly $\Delta\chi_3 = \chi_3(T_c^-) - \chi_3(T_c^+)$ that tracks closely with the structure of the specific heat [8, 9]. The non-spinflip ($\Delta J_z = 0$) magnetic excitations seen in both inelastic neutron scattering [10] and in Raman measurements [11, 12] also have Ising character, despite the absence of local moments at those temperatures and pressures. Finally, quantum oscillations measured deep within the HO region indicate a quasiparticle g-factor with strong Ising anisotropy, $g(\theta) \propto \cos\theta$, where θ is the angle away from the c-axis [13, 14]. This $g(\theta)$ is confirmed by upper critical field experiments [15], that indicate that Ising quasiparticles pair to form a Pauli-limited superconductor. In this paper, we present a bulk thermodynamic measurement of the Ising

nature of the hidden order parameter, which shows that this Ising anisotropy is present not only deep inside the HO, but at the transition itself; it is even present in the order parameter fluctuations above T_c .

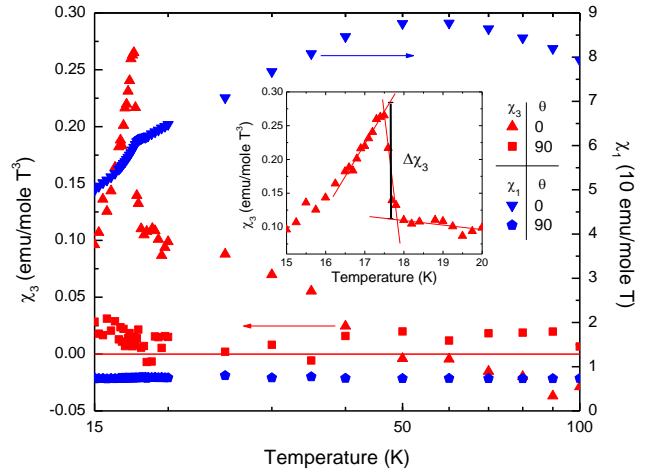


FIG. 1. Showing linear and nonlinear susceptibility versus temperature for fields along the c-axis ($\theta = 0^\circ$) and in the basal plane ($\theta = 90^\circ$).

As a rank-4 tensor, the nonlinear susceptibility χ_{3abcd} ,

$$M^a = \chi_{1ab}H^b + \frac{1}{3!}\chi_{3abcd}H^bH^cH^d \quad (1)$$

is particularly well-suited to probe symmetry-allowed anisotropies in the tetragonal crystal environment (space group $I4/mmm$) of URu₂Si₂; here M and H refer to the magnetization and the applied magnetic field respectively, and we use a summation convention for repeated

indices. In this paper we present an angular survey of the HO transition, reporting an extensive series of nonlinear susceptibility $[\chi_3(\theta, \phi)]$ measurements. Our results have important implications for the nature of the quasiparticles in the HO phase, and we also use $\chi_3(\theta, \phi)$ to probe the angular anisotropy of short-range order parameter fluctuations at temperatures above the HO transition.

The general expression for the field-dependent part of the free energy in a tetragonal crystal at fixed temperature is

$$F = -\chi_1(\theta) \frac{H^2}{2} - \chi_3(\theta, \phi) \frac{H^4}{4!} \quad (2)$$

with

$$\begin{aligned} \chi_1(\theta) &= \chi_1^a + \chi_1^b \cos^2 \theta \quad \text{and} \\ \chi_3(\theta, \phi) &= \chi_3^a + \chi_3^b \cos^2 \theta + \chi_3^c \cos^4 \theta + \chi_3^d \sin^4 \theta \sin^2 2\phi \end{aligned} \quad (3)$$

where θ and ϕ refer to the angles away from the c-axis and in the basal plane respectively; details of this angular decomposition are in the Supplementary Material. The anomaly in $\Delta\chi_3$ is a known signature of HO [9]. Because there is no Van Vleck contribution to the anomaly $\Delta\chi_3$, it is a direct thermodynamic probe of the g-factor at the HO transition. A key question is whether the anisotropic g-factor found in quantum oscillations persists to higher temperatures in the hidden order phase. Consistency with the low-temperature $g(\theta) \propto \cos \theta$ results requires a large change in χ_3^c , $\Delta\chi_3^c$, and negligible $\Delta\chi_3^a$ and $\Delta\chi_3^b$.

The URu_2Si_2 crystal used in this study is of dimension $4\text{mm} \times 2.5\text{mm} \times 2\text{mm}$ and has been previously described [9, 16]. A recent measurement of $C(T)$ as well as the χ_1 and χ_3 measurements reported here show no change in these properties over time [9]. The narrow width of the specific heat transition, $\Delta T_{HO} = 0.35\text{K}$ is consistent with high quality samples of comparable dimensions [17–19]. Additionally, the single superconducting transition indicates a single phase [16] confirming the high quality of the sample. Measurements of the magnetization, M , were performed in a commercial superconducting quantum interference device (SQUID) magnetometer, as a function of temperature (T), magnetic field (H), and angle (θ) between the sample's c-axis and H . The variation in angle was achieved with a set of sample mounts machined from Stycast 1266 epoxy. The linear and leading nonlinear (χ_3) susceptibilities were determined as in [9]. Multiple measurements (~ 1800 M(H) scans) were performed with sufficient resolution in H , T and θ to resolve the angular dependence of the χ_3 discontinuity at T_c . Values for $\Delta\chi_3$ were obtained at every θ using a straight-line construction assuming a mean-field jump at T_c .

Figure 1 shows $\chi_1(T)$ and $\chi_3(T)$ as a function of temperature at $\theta = 0^\circ$ and 90° , data that agree well with previous reports [9]. We note that the nonlinear susceptibility displays a sharp anomaly at the HO transition,

whereas $\chi_1(T)$ displays a corresponding discontinuity in its gradient $d\chi_1(T)/dT$; both χ and χ_3 are significantly larger for $\theta = 0^\circ$ (c-axis) than for $\theta = 90^\circ$ (ab plane).

In Figure 2 we show the angular dependence of $\Delta\chi_3$ and of χ_1 just above the HO transition. The linear susceptibility displayed in figure 2 is characterized by the form

$$\chi_1(\theta, T) = \chi_1^{(0)} + \chi_1^{Ising}(T) \cos^2 \theta, \quad (4)$$

where the isotropic component $\chi_1^{(0)}$ of the susceptibility displays no discernable temperature dependence. The temperature-dependent Ising component, χ_1^{Ising} displays a discontinuity $\frac{d\chi_1^{Ising}}{dT}$ at the HO transition. Whereas $\chi_1(\theta)$ varies as $\cos^2 \theta$ at $T = 18\text{K}$, in Fig. 2 the sharp jump in χ_3 at the transition, $\Delta\chi_3$ has a distinctive $\cos^4 \theta$ dependence

$$\Delta\chi_3(\theta, \phi) = \Delta\chi_3^{Ising} \cos^4 \theta \quad (5)$$

without any constant (Van Vleck) terms; this then indicates that $\Delta\chi_3^c \gg \Delta\chi_3^b, \Delta\chi_3^a$ in (4), consistent with the low-temperature $g(\theta)$ measurements. We note that, within experimental resolution, no χ_3^d component was observed in the measurements, either above or at the transition.

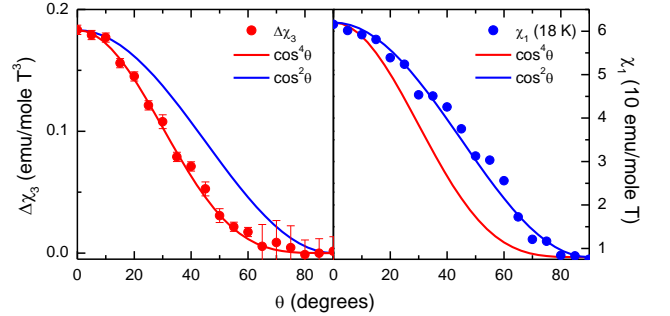


FIG. 2. Angular dependence of (a) the jump $\Delta\chi_3$ in the nonlinear susceptibility at the hidden order transition and (b) the magnetic susceptibility just above the hidden order transition at 18K.

In Figure 3 we compare the angular dependences of $\Delta\chi_3$ with $\chi_3(18\text{K})$, $\chi_3(30\text{K})$ and $\chi_3(100\text{K})$, just above, moderately above and well above T_c . At 18 K and 30 K, χ_3 follows $\cos^4 \theta$, similar to $\Delta\chi_3$. At 100 K, the positive contribution to χ_3 associated with the HO transition has completely vanished, leaving a negative response presumably associated with single-ion dipolar physics; the signal is too small to resolve the anisotropy. At $T = 18\text{K}$, χ_3 is about 1.6 times smaller than $\Delta\chi_3$, (c.f. Fig. 1), and is well described by the form

$$\chi_3(\theta, T) = \chi_3^{(0)} + \chi_3^{Ising}(T) \cos^4 \theta, \quad (6)$$

where the isotropic component $\chi_3^{(0)}$ is essentially temperature-independent. A $\cos^4 \theta$ dependence in $\chi_3(T)$

is still observed at 30K, and by comparing the c-axis and basal plane measurements, we estimate that around 60K, $\chi_3^{Ising}(T)$ goes to zero (see Fig. 1). Above 100K, the $\cos^4 \theta$ dependence is no longer discernable, leading us to infer that the Ising component of the nonlinear susceptibility vanishes around 60K.

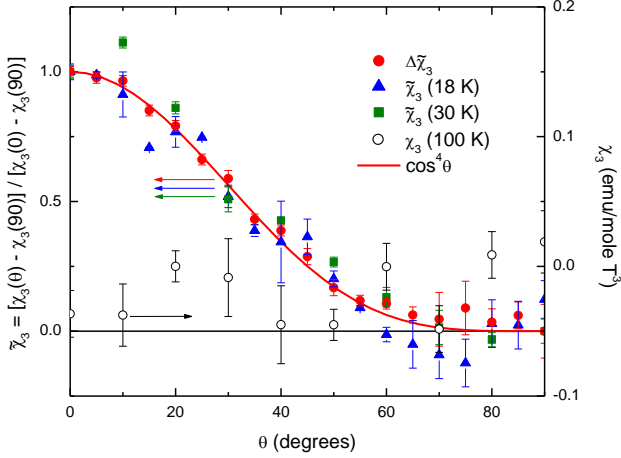


FIG. 3. Angular dependence of $\Delta\chi_3$ and χ_3 at three different temperatures, showing the disappearance of the Ising behavior at high temperatures.

At the HO transition, our results can be analyzed within a minimal Landau free energy density of the form

$$f(T, \psi) = a(T - T_c(H))\psi^2 + \frac{b}{2}\psi^4 \quad (7)$$

where we describe a domain of hidden order by a real order parameter ψ and

$$T_c(H) = T_c - \frac{1}{2}Q_{ab}H_aH_b + O(H^4) \quad (8)$$

defines the leading field-dependent anisotropy in the transition temperature, where Q_{ab} is a tensor capturing how the order parameter ψ couples to magnetic field; experimental consequences of (7) [9] are discussed in the Supplementary Material. The quantity $\Delta\chi_{ab} = -aQ_{ab}\psi^2$ is the magnetic susceptibility associated with the hidden order. By minimizing the free energy with respect to ψ , the free energy below T_c is then $f(T) = -(a^2/2b)[T_c(H) - T]^2$. The jump in the linear and nonlinear susceptibilities are then given by

$$\left(\Delta \frac{d\chi_1}{dT}\right)_{ab} = -\frac{a^2}{b}Q_{ab} \quad (9)$$

$$(\Delta\chi_3)_{abcd} = \frac{a^2}{b}(Q_{ab}Q_{cd} + Q_{ac}Q_{bd} + Q_{ad}Q_{cb}). \quad (10)$$

In order to determine the robustness of the Ising anisotropy, by setting $Q_{xx} = Q_{yy} = \Phi Q_{zz}$, we codify

our results in terms of an angle-dependent coupling between the hidden order parameter ψ and the magnetic field of the form

$$\Delta f[\psi, \theta] = -\frac{aQ_{zz}}{2}\psi^2 H^2(\cos^2 \theta + \Phi \sin^2 \theta), \quad (11)$$

where Φ quantifies the fidelity of the Ising-like behavior, so that $\Phi = 0$ and $\Phi = 1$ correspond to Ising and isotropic behavior respectively. The corresponding jump in the nonlinear susceptibility at T_c is

$$\Delta\chi_3(\theta) \propto (\cos^2 \theta + \Phi \sin^2 \theta)^2. \quad (12)$$

Our measurements indicate a very small $\Phi = 0.036 \pm 0.021$, as shown in figure 4 (inset), where details of the fitting procedure are given in the Supplementary Materials. Such a small value of Φ could be accounted for by an angular offset of only one degree, via equation 24. X-ray diffraction orientation measurements indicate an uncertainty in the c-axis of our sample of no more than $\pm 3^\circ$. In figure 4, one can see that this value provides upper and lower bounds to the $\cos^4 \theta$ -dependence of $\Delta\chi_3$ that bracket the data symmetrically. Thus, a Φ value of 0.036 is well below the total uncertainty of the measurement. To reduce the uncertainty in Φ even further would require angular accuracy of well below 1° , which is beyond the capability of the present apparatus. Thus, the obtained $\Phi = 0.036$ is consistent also with $\Phi = 0$.

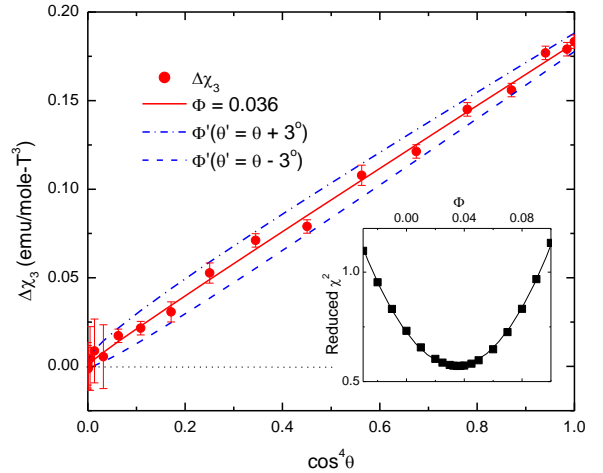


FIG. 4. $\Delta\chi_3$ as a function of $\cos^4 \theta$, fit to equation 24 for different values of Φ . Blue dashed lines indicate Φ -values assuming an angular offset of 3° ($\theta' = \theta \pm 3^\circ$). Inset shows the effect of Φ on the goodness of fit, expressed as the reduced χ^2 (see Supplementary Material).

We now discuss the implications of these results. At the very simplest level, our results show that the free energy of URu_2Si_2 only depends on the z component of the magnetic field, i.e. $F[\vec{H}] = F[H_z]$. In particular:

- The coupling of the order parameter to the magnetic field involves an Ising coupling $F[H, \psi] = -\frac{1}{2}Q_{zz}\psi^2 H_z^2$ coupling.
- In the microscopic Hamiltonian, the Zeeman coupling of the magnetic field is strongly Ising, with the field coupling to the z-component of the total angular momentum $-J_z B_z$.

The second point follows because derivatives of the free energy with respect to field are equivalent, inside the trace of the partition function, to the magnetization operator $-\frac{\delta}{\delta H_z} \equiv \hat{M}_z$, so that if the free energy only depends on H_z , the partition function $Z = \text{Tr} e^{-\beta H}$ and hence the Hamiltonian only depends on $\hat{M}_z = g\hat{J}_z$.

However, these simple conclusions have implications for the microscopic physics. On the one hand, we can link the Ising anisotropy of the microscopic Hamiltonian to the single-ion properties of the U ions in URu_2Si_2 , where the Zeeman coupling $-g_f\mu_B J_z B_z$ is a sign of vanishing matrix elements $\langle +|J_\pm|-\rangle = 0$. From a single-ion standpoint, an almost perfect Ising anisotropy is a strong indication of an *integer spin* $5f^2 U^{4+}$ ground-state with $J = 4$. High-spin Ising configurations of the alternative $5f^3 U^{3+}$ ionic configurations are ruled out because the coupling of the local moment to the tetragonal environment mixes configurations by adding angular momenta in units of $\pm 4\hbar$, for example $J_z = \pm 5/2$ and $\mp 3/2$, leading almost inevitably to a non-zero transverse Zeeman coupling when the angular momentum J is half-integer. Although the precise crystal-field configuration of the U ions is still uncertain [20–22], both dynamical mean-field calculations [23] and high-resolution RIXS measurements [21] confirm the predominantly $5f^2$ picture.

Yet a single-ion picture is not enough, for the sharpness of the specific-heat anomaly, the sizable entropy and the gapping of two-thirds of the Fermi surface associated with the hidden order transition [1] all suggest an underlying *itinerant* ordering process. The remarkable feature of our data is that the jump $\Delta\chi_3$ that reflects the itinerant ordering process exhibits a strong Ising anisotropy. This result links in with the observation of multiple spin zeroes in dHvA measurements, which detect the presence of itinerant heavy quasiparticles with an Ising g-factor $g(\theta) = g_f \cos \theta$ at low temperatures. Our new results suggest that these same quasiparticles survive all the way up to the hidden order transition. In the Landau theory, we can identify the Ising-like coupling between HO and the magnetic field in terms of the squared g-factor $Q_{zz}\psi^2 \cos^2 \theta \propto g(\theta)^2 \psi^2$.

Reconciling the single-ion and itinerant perspectives, both supported strongly by experiment, poses a fascinating paradox. The simplest possibility is that the Ising anisotropy of the f-electrons is a one-electron effect resulting from a renormalized, spin-orbit coupled f-band that develops at temperatures well above the hidden order transition. In this purely itinerant view, the hidden

order is a multipolar density wave that develops within a pre-formed band of Ising quasiparticles [24, 25]. Microscopically such quasiparticles are renormalized one-particle f-orbitals formed from high-spin orbitals with half-integer $|J_z|$. Provided only one $|J_z| > 1/2$ is involved, the transverse matrix elements of the angular momentum operator $\langle \pm | J_\pm | \pm \rangle = 0$ identically vanish, leading to a perfect Ising anisotropy. Such Ising quasiparticles have been observed in strong spin-orbit coupled systems, but only at high symmetry points in the Brillouin zone [26]. Moreover, in a tetragonal environment, when an electron resonantly scatters off an f-state, J_z is only conserved mod(4). Thus a mobile heavy Bloch wave must actively exchange $\pm 4\hbar$ units of angular momentum as it propagates through the lattice, leading to Bloch states composed of a mixture of J_z states, such as

$$|\mathbf{k}\pm\rangle = \alpha|\mathbf{k}, \pm 5/2\rangle + \beta|\mathbf{k}, \mp 3/2\rangle. \quad (13)$$

This inevitably gives rise to a finite transverse coupling and a finite Φ in the phenomenological Landau theory, ($\Phi \propto |\alpha\beta|^2$) that is ruled out by these experiments.

An alternative is that the itinerant f-quasiparticles carry *integer* angular momentum, inheriting the Ising anisotropy of a localized $5f^2$ local moment of the U atoms via a phase transition rather than a crossover. In this scenario, even though J_z is conserved mod(4), Ising anisotropy is preserved since the up-spin and down-spin configurations differ by at least two units of angular momentum. However, this picture requires that the half-integer conduction electrons hybridize with the underlying integer f-states, which can only occur in the presence of a spinorial or “hastatic” order parameter [27–30]. Indeed, the hastatic order scenario predicted the $\Delta\chi_3 \propto \cos^4 \theta$ observed in this experiment, although theoretical efforts to develop a microscopic theory of hastatic order predicted a small transverse moment that has been shown to be absent in high-precision neutron scattering experiments [31–33]. The vanishing of the anisotropy constant ($\Phi = 0$) in our nonlinear susceptibility measurements combined with the null result reported by neutron scattering represents a fascinating challenge to our future understanding of hidden order.

The continuation of the Ising anisotropy well above T_c is also remarkable. While single-ion physics can give a negative Ising anisotropic χ_3 , for an isolated Ising ground state doublet, or a positive, but more isotropic χ_3 , if there are several singlets in the temperature range of interest, there is no way to explain the positive Ising anisotropic χ_3 emerging below 60K with single ion physics. Instead, this response indicates Ising anisotropic order parameter fluctuations extending up to more than three times T_c , an extraordinarily large fluctuation regime.

An interesting question raised by our work is whether bulk nonlinear susceptibility measurements can be used to detect microscopic broken tetragonal symmetry that

has been reported in torque magnetometry measurements [2]. In principle, were the hidden order to possess domains with broken tetragonal symmetry, inter-domain fluctuations in the basal-plane susceptibility would manifest themselves through a finite value of χ_3^d below T_c . The large Ising anisotropy suppresses the precision for in-plane susceptibility measurement: our current work places an upper bound on the microscopic symmetry-breaking susceptibility $|\Delta\chi_{xy}|$ such that $|\Delta\chi_{xy}|/\chi_{xx} \leq 1$ that is two orders of magnitude larger than that measured by torque magnetometry on μm size samples [2] (see Supplementary Materials), and thus our negative results are not inconsistent with their positive finding. However improvement in resolution in future measurements could make it possible to address this issue.

In summary, we have presented a detailed survey of the nonlinear magnetic susceptibility as a function of angle and temperature in the hidden order compound URu_2Si_2 . These measurements showcase the unique Ising anisotropy, and imply that it is a key feature of the hidden order parameter. While previous quantum oscillation measurements indicated the presence of Ising quasiparticles, this Ising anisotropy persists not only to the transition temperature, but all the way up to 60K, putting serious constraints on the theory of hidden order. It would be quite interesting to examine the nonlinear susceptibility anisotropy in and above the antiferromagnetic phase, which could be done in $\text{URu}_{2-x}\text{Fe}_x\text{Si}_2$ [34].

Acknowledgments: This work was supported by National Science Foundation grants NSF DGE 1339067 (J. Trinh), NSF DMR-1334428 (P. Chandra), NSF DMR 1309929 (P. Coleman), NSF DMR 1534741 (A.P. Ramirez) and Ames Laboratory Royalty Funds and Iowa State University startup funds (R. Flint). The Ames Laboratory is operated for the U.S. Department of Energy by Iowa State University under Contract No. DE-AC02-07CH11358. PC, PC and and RF acknowledge the hospitality of the Aspen Center for Physics, supported by NSF PHYS-1066293, where early parts of this work were discussed. TS acknowledges funding by the U.S. Department of Energy, Office of Basic Energy Sciences, Materials Sciences and Engineering Division, under award No. DE-SC0008832. P. Chandra thanks S. Bahramy for a stimulating discussion on Ising quasiparticles in MoS_2 .

-
- [1] J. Mydosh and P. M. Oppeneer, “Colloquium: Hidden Order, Superconductivity and Magnetism – The Unsolved Case of URu_2Si_2 ,” *Reviews of Modern Physics*, 1–23 (2011).
 - [2] R. Okazaki, T. Shibauchi, H.J. Shi, Y. Haga, T. D. Matsuda, E. Yamamoto, Y. Onuki, H. Ikeda, and Y. Matsuda, “Rotational Symmetry Breaking in the Hidden Order Phase of URu_2Si_2 ,” *Science*, 349–442 (2011).
 - [3] S. Tonegawa, K. Hashimoto, K. Ikada, Y.-H. Lin, H. Shishido, Y. Haga, T. D. Matsuda, E. Yamamoto, Y. Onuki, H. Ikeda, Y. Matsuda, and T. Shibauchi, “Cyclotron Resonance in the Hidden-Order Phase of URu_2Si_2 ,” *Phys. Rev. Lett.* **109**, 036401 (2012).
 - [4] S. Tonegawa, S. Kasahara, T. Fukuda, K. Sugimoto, N. Yasuda, Y. Tsuruhara, D. Watanabe, Y. Mizukami, Y. Haga, T. D. Matsuda, E. Yamamoto, Y. Onuki, H. Ikeda, Y. Matsuda, and T. Shibauchi, “Direct Observation of Lattice Symmetry Breaking at the Hidden-Order Transition in URu_2Si_2 ,” *Nat. Comm.* **5**, 4188 (2014).
 - [5] S.C. Riggs, M.C. Shapiro, A. V. Maharaj, S. Raghu, E.D. Bauer, R.E. Baumbach, P. Giraldo-Gallo, M. Wartenbe, and I.R. Fisher, “Evidence for a Nematic Component to the Hidden-Order Parameter in URu_2Si_2 from Differential Elastoresistance Measurements,” *Nature Communications* **6**, 6425 (2015).
 - [6] T. Mito, M. Hattori, G. Motoyama, Y. Sakai, T. Koyama, K. Ueda, T. Kohara, M. Yokoyama, and H. Amitsuka, “Investigation of Local Symmetries in the Hidden-Order Phase of URu_2Si_2 ,” *J. Phys. Soc. Japan* **82**, 123704 (2013).
 - [7] S. Kambe, T. Tokunaga, and R.E. Walstedt, “Distributed Twofold Ordering in URu_2Si_2 ,” *Phys. Rev. B* **91**, 035111 (2015).
 - [8] Y. Miyako, S. Kawarazaki, H. Amitsuka, C.C. Paulsen, and K. Hasselbach, “Magnetic Properties of $\text{U}(\text{Ru}_{1-x}\text{Rh}_x)_2\text{Si}_2$ Single Crystals ($0 \leq x \leq 1$),” *J. Appl. Phys.* **70**, 2680 (1991).
 - [9] A.P. Ramirez, P. Coleman, P. Chandra, A.A. Menovsky, Z. Fisk, and E. Bucher, “Nonlinear Susceptibility as a Probe of Tensor Order in URu_2Si_2 ,” *Phys. Rev. Lett.* **68**, 2680 (1992).
 - [10] C. Broholm, H. Lin, P.T. Matthews, T. E. Mason, W. J. L. Buyers, M. F. Collins, A. A. Menovsky, J. A. Mydosh, and J. K. Kjems, “Magnetic Excitations in the Heavy-Fermion Superconductor URu_2Si_2 ,” *Phys. Rev. B* **43**, 12809–12822 (1991).
 - [11] J. Buhot, M.-A. Measson, Y. Gallais, M. Cazayous, A. Sacuto, G. Lapertot, and D. Aoki, “Symmetry of the Excitations in the Hidden Order State in URu_2Si_2 ,” *Phys. Rev. Lett.* **113**, 266405 (2015).
 - [12] H.-H. Kung, R.E. Baumbach, E. Bauer, V.K. Thorsmolle, W.L. Zhang, K. Haule, J.A. Mydosh, and G. Blumberg, “Chirality Density Wave of the Hidden Order Phase in URu_2Si_2 ,” *Science* **347**, 1339 (2015).
 - [13] H. Ohkuni, Y. Inada, Y. Tokiwa, K. Sakurai, R. Settai, T. Honma, Y. Haga, E. Yamamoto, Y. Nuki, and H. Yamagami, “Fermi Surface Properties and de Haas–van Alphen Oscillation in Both the Normal and Superconducting Mixed States of URu_2Si_2 ,” *Philosophical Magazine B* **79**, 1045–1077 (1999).
 - [14] M. M. Altarawneh, N. Harrison, S. E. Sebastian, L. Balicas, P. H. Tobash, J. D. Thompson, F. Ronning, and E. D. Bauer, “Sequential Spin Polarization of the Fermi Surface Pockets in URu_2Si_2 and Its Implications for Hidden Order,” *Phys. Rev. Lett.* **106**, 146403 (2011).
 - [15] M. Altarawneh, N. Harrison, G. Li, L. Balicas, P. Tobash, F. Ronning, and E. Bauer, “Superconducting Pairs with Extreme Uniaxial Anisotropy in URu_2Si_2 ,” *Phys. Rev. Lett.* **108**, 066407 (2012).
 - [16] A. P. Ramirez, T. Siegrist, T. T. M. Palstra, J. D. Garrett, E. Bruck, A. A. Menovsky, and J. A. Mydosh, “Superconducting Phases of URu_2Si_2 ,” *Phys. Rev. B* **44**, 5392–5395 (1991).
 - [17] T.D. Matsuda, E. Hassinger, D. Aoki, V. Taufour,

- G. Knebel, T. Naoyuki, Y. Etsuji, Y. Haga, Y. Onuki, Z. Fisk, and J. Flouquet, “Details of Sample Dependence and Transport Properties of URu_2Si_2 ,” *J. Phys. Soc. Japan* **80**, 114710 (2011).
- [18] S. Kambe, Y. Tokunaga, H. Sakai, T. D. Matsuda, Y. Haga, Z. Fisk, and R. E. Walstedt, “NMR Study of In-Plane Twofold Ordering in URu_2Si_2 ,” *Phys. Rev. Lett.* **110**, 246406 (2013).
- [19] P. G. Niklowitz, S. R. Dunsiger, C. Pfleiderer, P. Link, A. Schneidewind, E. Faulhaber, M. Vojta, Y.-K. Huang, and J. A. Mydosh, “Role of Commensurate and Incommensurate Low-Energy Excitations in the Paramagnetic to Hidden-Order Transition of URu_2Si_2 ,” *Phys. Rev. B* **92**, 115116 (2015).
- [20] J. R. Jeffries, K. T. Moore, N. P. Butch, and M. B. Maple, “Degree of $5f$ electron localization in ur_2si_2 : Electron energy-loss spectroscopy and spin-orbit sum rule analysis,” *Phys. Rev. B* **82**, 033103 (2010).
- [21] L. A. Wray, J. Denlinger, S.-W. Huang, H. He, N. P. Butch, M. B. Maple, Z. Hussain, and Y.-D. Chuang, “Spectroscopic Determination of the Atomic f -Electron Symmetry Underlying Hidden Order in URu_2Si_2 ,” *Phys. Rev. Lett.* **114**, 236401–6 (2015).
- [22] C. H. Booth, S. A. Medling, J. G. Tobin, R. E. Baumbach, E. D. Bauer, D. Sokaras, D. Nordlund, and T.-C. Weng, “Probing $5f$ -state configurations in ur_2si_2 with u L_{III} -edge resonant x-ray emission spectroscopy,” *Phys. Rev. B* **94**, 045121 (2016).
- [23] K. Haule and G. Kotliar, “Arrested Kondo Effect and Hidden Order in URu_2Si_2 ,” *Nature Physics* **5**, 796–799 (2009).
- [24] J. Rau and H.-Y. Kee, “Hidden and Antiferromagnetic Order as a Rank-5 Superspin in URu_2Si_2 ,” *Phys. Rev. B* **85**, 245112 (2012).
- [25] H. Ikeda, M.-T. Suzuki, R. Arita, T. Takimoto, T. Shibauchi, and Y. Matsuda, “Emergent Rank-5 Nematic Order in URu_2Si_2 ,” *Nature Physics* **8**, 528–533 (2012).
- [26] Y. Saito, Y. Nakamura, M. S. Bahramy, Y. Kohama, J. Ye, Y. Kasahara, Y. Nakagawa, M. Onga, M. Tokunaga, T. Nojima, Y. Yanase, and Y. Iwasa, “Superconductivity Protected by Spin-Valley Locking in Ion-Gated MoS_2 ,” *Nature Physics* **12**, 144–149 (2016).
- [27] P. Chandra, P. Coleman, and R. Flint, “Hastatic Order in the Heavy-Fermion Compound URu_2Si_2 ,” *Nature* **493**, 621–626 (2013).
- [28] R. Flint, P. Chandra, and P. Coleman, “Hidden and Hastatic Orders in URu_2Si_2 ,” *Journal of the Physical Society of Japan* **83**, 061003 (2014).
- [29] P. Chandra, P. Coleman, and R. Flint, “Ising Quasiparticles and Hidden Order in URu_2Si_2 ,” *Philosophical Magazine* **94**, 3803–3819 (2014).
- [30] P. Chandra, P. Coleman, and R. Flint, “Hastatic Order in URu_2Si_2 : Hybridization with a Twist,” *Physical Review B* **91**, 205103 (2015).
- [31] P. Das, R. E. Baumbach, K. Huang, M. B. Maple, Y. Zhao, J. S. Helton, J. W. Lynn, E. D. Bauer, and M. Janoschek, “Absence of a Static In-Plane Magnetic Moment in the ‘Hidden-Order’ Phase of URu_2Si_2 ,” *New Journal of Physics* **15**, 053031 (2013).
- [32] N. Metoki, H. Sakai, E. Yamamoto, N. Tateiwa, T. Matsuda, and Y. Haga, “Neutron Scattering Experiments for the Study of In-Plane Ordered Moment in URu_2Si_2 ,” *Journal of the Physical Society of Japan* **82**, 055004 (2013).
- [33] K. A. Ross, L. Harriger, Z. Yamani, W. J. L. Buyers, J. D. Garrett, A. A. Menovsky, J. A. Mydosh, and C. L. Broholm, “Strict Limit on In-Plane Ordered Magnetic Dipole Moment in URu_2Si_2 ,” *Phys. Rev. B* **89**, 155122 (2014).
- [34] N. Kanchanavatee, M. Janoschek, R. E. Baumbach, J. J. Hamlin, D. A. Zocco, K. Huang, and M. B. Maple, “Twofold enhancement of the hidden-order/large-moment antiferromagnetic phase boundary in the $\text{URu}_{2-x}\text{Fe}_x\text{Si}_2$ system,” *Phys. Rev. B* **84**, 245122 (2011).

SUPPLEMENTARY MATERIAL FOR “THERMODYNAMIC MEASUREMENT OF ANGULAR ANISOTROPY AT THE HIDDEN ORDER TRANSITION OF URU₂SI₂”

ANGULAR DECOMPOSITION OF χ_3 IN A TETRAGONAL ENVIRONMENT

The expansion of the Free energy as a function of magnetic field strength H can be written

$$\Delta F = -\frac{1}{2}H_a H_b \chi_{ab}^1 - \frac{1}{4!}H_a H_b H_c H_d \chi_{abcd}^3 \quad (14)$$

The fourth order coupling to the field can be treated in a fashion closely analogous to the elastic free energy of a material, χ_{abcd}^3 playing the role of the elasticity tensor C_{abcd} , with the additional proviso that χ_{abcd}^3 is a completely symmetric tensor. In a tetragonal crystal with mirror symmetries, the only non-vanishing components of the nonlinear susceptibility tensor are

$$\begin{aligned} \chi_{1111} &= \chi_{2222}, \\ \chi_{3333} & \\ \chi_{1122} &= \chi_{1212}, \\ \chi_{1133} &= \chi_{2233} = \chi_{1313} = \chi_{2323}. \end{aligned} \quad (15)$$

The fourth order contribution to the nonlinear susceptibility can then be written as

$$\begin{aligned} \Delta F_4 &= -\frac{1}{4!}H_a H_b H_c H_d \chi_{abcd}^3 \\ &= -\frac{1}{4!} [\chi_{1111}(H_x^4 + H_y^4) + \chi_{3333}H_z^4 + 6\chi_{1122}H_x^2 H_y^2 + 6\chi_{1133}(H_x^2 + H_y^2)H_z^2] \end{aligned} \quad (16)$$

Substituting $(H_1, H_2, H_3) \rightarrow H(\sin \theta \cos \phi, \sin \theta \sin \phi, \cos \theta)$, we obtain

$$\begin{aligned} \Delta F &= -\frac{H^4}{4!} \left(\chi_{1111}(1 - \cos^2 \theta)^2(1 - \frac{1}{2} \sin^2 2\phi) + \chi_{3333} \cos^4 \theta \right. \\ &\quad \left. + \frac{6}{4} \chi_{1122} \sin^4 \theta \sin^2 2\phi + 6\chi_{1133}(1 - \cos^2 \theta) \cos^2 \theta \right) \\ &= -\frac{H^4}{4!} (\chi_3^a + \chi_3^b \cos^2 \theta + \chi_3^c \cos^4 \theta + \chi_3^d \sin^4 \theta \sin^2 2\phi) \end{aligned} \quad (17)$$

where

$$\begin{aligned} \chi_3^a &= \chi_{1111}, \\ \chi_3^b &= 6\chi_{1133} - 2\chi_{1111} \\ \chi_3^c &= \chi_{1111} + \chi_{3333} - 6\chi_{1133} \\ \chi_3^d &= \frac{1}{2}(-\chi_{1111} + 3\chi_{1122}). \end{aligned} \quad (18)$$

LANDAU THEORY FOR THE MINIMAL FREE ENERGY

In this section, we further document the experimental consequences of our minimal Landau free energy, as has already been explored in Ramirez et al[1]. If we take the free energy,

$$f[T, \psi] = a(T - T_c + \frac{1}{2}Q_{zz}H_z^2)\psi^2 + \frac{b}{2}\psi^4, \quad (19)$$

and solve for $\psi^2(T, H_z) = a^2(T_c - \frac{1}{2}Q_{zz}H_z^2 - T)^2/b$, we find the free energy below T_c ,

$$f[T] = -\frac{a^2}{2b}(T_c - \frac{1}{2}Q_{zz}H_z^2 - T)^2. \quad (20)$$

We can then take the appropriate derivatives to obtain the jumps in the specific heat, $d\chi_1/dT$ and χ_3 at T_c in zero field,

$$\frac{\Delta C_V}{T_c} = \frac{a^2}{b}; \quad \Delta \frac{d\chi_1}{dT} = \frac{a^2 Q_{zz}}{b}; \quad \Delta \chi_3 = \frac{3a^2 Q_{zz}^2}{b}. \quad (21)$$

These jumps obey the thermodynamic relation,

$$\frac{\Delta C_V}{T} \Delta \chi_3 = 12 \left(\frac{d\chi_1}{dT} \right)^2. \quad (22)$$

As these quantities have been measured for hidden order ($\frac{\Delta C_V}{T_{HO}} = 300$ mJ/mol K²[2] and $\Delta \chi_3 = 1.8$ emu/mol T³, we can estimate,

$$Q_{zz} = \sqrt{\frac{\Delta \chi_3 T_{HO}}{3 \Delta C_V}} = .04 \text{K/T}^2. \quad (23)$$

If one neglects higher order corrections to $T_c(H_z) = T_c - \frac{1}{2} Q_{zz} H_z^2 + O(H_z^4)$, this value of Q_{zz} means that T_c would vanish around 28T, which is roughly consistent with the experimental value[3], even though higher order terms will certainly be important at those high fields.

ANGULAR FITTING PROCEDURE FOR $\Delta \chi_3(\theta)$

We assumed a fit for $\Delta \chi_3$ of the form

$$\Delta \chi_3(\theta) \propto (\cos^2 \theta + \Phi \sin^2 \theta)^2. \quad (24)$$

and determined Φ by optimizing the goodness of fit, or by minimizing the reduced χ^2 of the fit, which is defined as the residual sum of squares weighted against the variance (square of the error) at each point, divided by the number of data points less the number of fit parameters,

$$\chi_{red}^2 = \sum_{i=1}^n \frac{\sigma^{-2} (\Delta \chi_{3meas}(\theta_i) - \Delta \chi_{3fit}(\theta_i))^2}{n - m}. \quad (25)$$

Here σ^2 is the variance, n is the number of data points and m is the number of fit parameters, which in this case is 1 since Φ is manually adjusted. Weighting against the variance allows us to incorporate the error in each $\Delta \chi_3$ measurement in our fit, while dividing by $n - m$ normalizes for the degrees of freedom.

The reduced χ^2 was calculated for several values of Φ , and the results are shown in the inset of Fig. 4 (main text), where the minimum as determined by a quadratic fit is $\Phi = 0.036 \pm 0.021$. As mentioned in the main text, an angular offset of one degree ($\theta' = \theta + 1^\circ$) is sufficient to account for this value of Φ when fitting to equation 24.

The intent behind using the reduced χ^2 is not to determine the goodness of fit relative to other models, but to extract an estimate for Φ and its error given the model that we propose. Thus, it is the robustness of the *minimum* of the reduced χ^2 that we require, not its absolute value. To ensure that our value of Φ is insensitive to random error, we have examined the effect of masking various points. The removal of any one point from the data set resulted in a change in Φ of ± 0.0013 on average, less than our uncertainty in Φ of 0.021.

Additionally, we compared our results with a similar analysis using other measures for goodness of fit (e.g., R^2) and found Φ -values within ± 0.0006 of 0.036, which is again within our error estimate.

ERROR BOUNDS ON THE IN-PLANE ANISOTROPY OF χ_3

Here we compute the bounds that our nonlinear susceptibility measurement place on the magnitude of the in-plane tetragonal symmetry breaking. For a single domain, broken tetragonal symmetry breaking manifests itself through the development of a finite off-diagonal component of the magnetic susceptibility, denoted by

$$\chi_{xy}^D \sim \left(\frac{V_D}{v_c} \right) \frac{\langle m_x m_y \rangle}{T}, \quad (26)$$

where V_D is the volume of the domain, v_c is the volume of a unit cell and $m_a = M_a/N_{cells}$ is the magnetization per cell. Now the bulk off-diagonal magnetic susceptibility involves an average over many different domains, which is zero:

$$\overline{\chi_{xy}} = 0, \quad (27)$$

where the overbar denotes a domain average. However, the domain fluctuations in the susceptibility remain finite, given by

$$\overline{(\Delta\chi_{xy})^2} = \left(\frac{V}{V_D}\right) (\chi_{xy}^D)^2, \quad (28)$$

where V is the total volume of the sample, and it is these fluctuations that give rise to a component of χ_3^d . Now the change in the bulk basal-plane nonlinear susceptibility (i.e in the ab-plane, perpendicular to the c axis) in the hidden order phase is then given by

$$\overline{\Delta\chi_\perp^3} \sim -\left(\frac{V}{v_c}\right) \frac{\overline{m_x m_y}^2}{T^3}. \quad (29)$$

Substituting in (26), we then obtain

$$\overline{\Delta\chi_\perp^3} \sim -\left(\frac{V v_c}{V_D^2}\right) \frac{(\chi_{xy}^D)^2}{T} = -\left(\frac{v_c}{V_D}\right) \frac{\overline{(\Delta\chi_{xy})^2}}{T} \quad (30)$$

Thus the inter-domain fluctuations in the symmetry-breaking component of the nonlinear susceptibility are expected to generate a contribution to $\Delta\chi_{xyxy}^3$.

To set bounds on this, we compare the anomalous basal-plane component of the nonlinear susceptibility with the nonlinear susceptibility along the z-axis, given by

$$\chi_{zzzz}^3 = \left(\frac{V}{v_c}\right) \frac{\langle m_z^4 \rangle}{T^3} \quad (31)$$

Now the susceptibility in the z-direction of a single domain is given by

$$\chi_{zz}^D = \frac{V_D}{v_c} \frac{\langle m_z^2 \rangle}{T}$$

so that we can write

$$\chi_{zzzz}^3 \sim \left(\frac{V}{v_c}\right) \left[\left(\frac{\chi_{zz}^D v_c}{V_D}\right) \right]^2 \frac{1}{T} \quad (32)$$

Taking the ratio of (30) and (32) we obtain

$$\frac{\overline{\Delta\chi_\perp^3}}{\chi_{zzzz}^3} = -\left(\frac{\chi_{xy}^D}{\chi_{zz}^D}\right)^2 = -\left(\frac{\chi_{xy}^D}{\chi_{xx}^D}\right)^2 \left(\frac{\chi_{xx}^D}{\chi_{zz}^D}\right)^2 = -\left(\frac{\chi_{xy}^D}{\chi_{xx}^D}\right)^2 \left(\frac{\chi_{xx}}{\chi_{zz}}\right)^2$$

where we have removed the superscript “ D ” in the ratio between basal-plane and c-axis susceptibilities in the last term. We thus see that the magnitude of the anomalous basal plane nonlinear susceptibility is substantially reduced by the squared ratio of the bulk basal-plane and c-axis susceptibilities.

We can rearrange this equation to set bounds on the in-plane tetragonality as follows:

$$\left| \frac{\chi_{xy}^D}{\chi_{xx}^D} \right| \leq \left(\frac{\chi_{zz}}{\chi_{xx}} \right) \sqrt{\left| \frac{\overline{\Delta\chi_\perp^3}}{\chi_{zzzz}^3} \right|} \quad (33)$$

Putting in numbers, the anisotropy in the linear susceptibility is at least five,

$$\left(\frac{\chi_{zz}}{\chi_{xx}} \right) > 5 \quad (34)$$

while the error bounds on the measurement of the in-plane nonlinear susceptibility are given by

$$\left| \frac{\overline{\Delta\chi_\perp^3}}{\chi_{zzzz}^3} \right| \leq 0.14 \quad (35)$$

so that

$$\left| \frac{\chi_{xy}^D}{\chi_{xx}^D} \right| \leq 5 \times \sqrt{0.14} \sim 1.9 \quad (36)$$

which sets a bound which is two orders of magnitude larger than the anisotropy measured by torque magnetometry in micron-sized tiny samples.

Thus there is no inconsistency between our nonlinear susceptibility measurement and previous torque magnetometry measurements. We also see that an order of magnitude improvement in the nonlinear susceptibility measurements would make it possible to observe the in-plane anisotropy using a bulk probe.

-
- [1] A. Ramirez, P. Coleman, P. Chandra, E. Brück, A. A. Menovsky, Z. Fisk, and B. E., Phys. Rev. Lett. **68**, 2680 (1992), URL [http://link.aps.org/doi/10.1103/](http://link.aps.org/doi/10.1103/PhysRevLett.68.2680)

-
- [PhysRevLett.68.2680](#).
 [2] T. Palstra, A. Menovsky, J. Berg, and A. Dirkmaat, Phys. Rev Lett. **55**, 2727 (1985).
 [3] K. H. Kim, N. Harrison, M. Jaime, G. S. Boebinger, and J. A. Mydosh, Phys. Rev. Lett. **91**, 256401 (2003), URL <http://link.aps.org/doi/10.1103/PhysRevLett.91.256401>.